Electronic Supplementary Material (ESI) for Nanoscale.

Supporting Information

Rethinking the Stability of Metal Nanoclusters: the Individual *versus* the Collective

Di Zhang,‡ Peiyao Pan,‡ Xiaoqin Du, Xi Kang,* Manzhou Zhu*

Department of Chemistry and Centre for Atomic Engineering of Advanced Materials, Anhui Province Key Laboratory of Chemistry for Inorganic/Organic Hybrid Functionalized Materials, Key Laboratory of Structure and Functional Regulation of Hybrid Materials, Anhui University, Ministry of Education, Anhui University, Hefei, Anhui 230601, P. R. China.

‡D.Z. and P.P. contributed equally to this work.
*E-mails of corresponding authors: kangxi_chem@ahu.edu.cn (X.K.); zmz@ahu.edu.cn (M.Z.)

This Supporting Information includes:

Experimental Details

Chemicals

Tetrachloroauric(III) acid ($HAuCl_4 \cdot 3H_2O$, 99.99%, metals basis), tetraoctylammonium bromide (TOAB, 98%,), Copper(II) acetylacetonate ($Cu(C_5H_7O_2)_2$, 99.99%, metals basis), sodium borohydride ($NaBH_4$, 99.99%), triphenylphosphine ($C_{18}H_{15}P$, 97%), 1-adamantanethiol ($C_{10}H_{15}SH$, 99%), toluene (Ph-CH_3, HPLC grade), methanol (CH_3OH, HPLC grade), methylene chloride (CH_2Cl_2, HPLC grade grade), *n*-hexane (C_6H_{14}, HPLC grade).

Synthesis of $Au_2Cu_6(S\text{-}Adm)_6(PPh_3)_2$ nanocluster (Au_2Cu_6-Triclinic)

$Au_2Cu_6(S\text{-}Adm)_6(PPh_3)_2$ was synthesized as reported previously (Angew. Chem. Int. Ed. 2016, 55, 3611). Briefly, $HAuCl_4 \cdot 3H_2O$ (0.1576 g, 0.4 mmol) and TOAB (0.2 g, 0.37 mmol) were dissolved in 15 mL of toluene and vigorously stirred for 15 minutes. Then, PPh_3 (0.3 g, 1.14 mmol; dissolved in 10 ml CH_3OH) was added. After 30 minutes, $Cu(C_5H_7O_2)_2$ (0.06 g, 0.23 mmol) was dissolved in 20 mL CH_3OH and added quickly. Then, Adm-SH (0.13g, 0.80 mmol; dissolved in 1 mL of toluene) and $NaBH_4$ (80mg, 2.1 mmol; dissolved in 1 mL of ice-cold water) were added simultaneously. The reaction was proceeded for 60 hours. The resulting solution was centrifuged to obtain the precipitate, which was washed several times with *n*-hexane. The precipitate was dissolved in the CH_2Cl_2 and toluene with *v*:*v* of 2:1, and underwent the crystallization with a liquid diffusion approach by diffusing the *n*-hexane (as depicted in Scheme S1). After three days, red crystals were obtained, and the crystal structure of the Au_2Cu_6-Triclinic nanocluster was determined.

Synthesis of $Au_2Cu_6(S\text{-}Adm)_6(PPh_3)_2$ nanocluster (Au_2Cu_6-Trigonal)

For the crystallization system of Au_2Cu_6-Triclinic, after another seven days, the red crystals gradually disappeared, and meanwhile, several small-sized black and rhombic crystals appeared at the bottom of the single-crystal culture plate, proven to be the Au_2Cu_6 with a trigonal crystalline system (i.e., Au_2Cu_6-Trigonal).

Characterizations

The optical absorption (UV-vis) spectra of nanoclusters were recorded using an Agilent 8453 diode array spectrometer.

Photoluminescence spectra were measured on a FLUOROLOG-3-TAU spectrometer.

X-Ray Crystallography

The data collection for single-crystal X-ray diffraction (SC-XRD) of all nanocluster crystal samples was carried out on Stoe Stadivari diffractometer under nitrogen flow, using graphite-monochromatized Cu Kα radiation (λ = 1.54186 Å). Data reductions and absorption corrections were performed using the SAINT and SADABS programs, respectively. The structure was solved by direct methods and refined with full-matrix least squares on F^2 using the SHELXTL software package. All non-hydrogen atoms were refined anisotropically, and all the hydrogen atoms were set in geometrically calculated positions and refined isotropically using a riding model. All crystal structures were treated with PLATON SQUEEZE. The CCDC number of the Au_2Cu_6-Triclinic nanocluster is 2347499. The CCDC number of Au_2Cu_6-Trigonal nanocluster is 2347507.

Scheme S1. The preparation, crystallization, and transformation of Au_2Cu_6 nanoclusters.

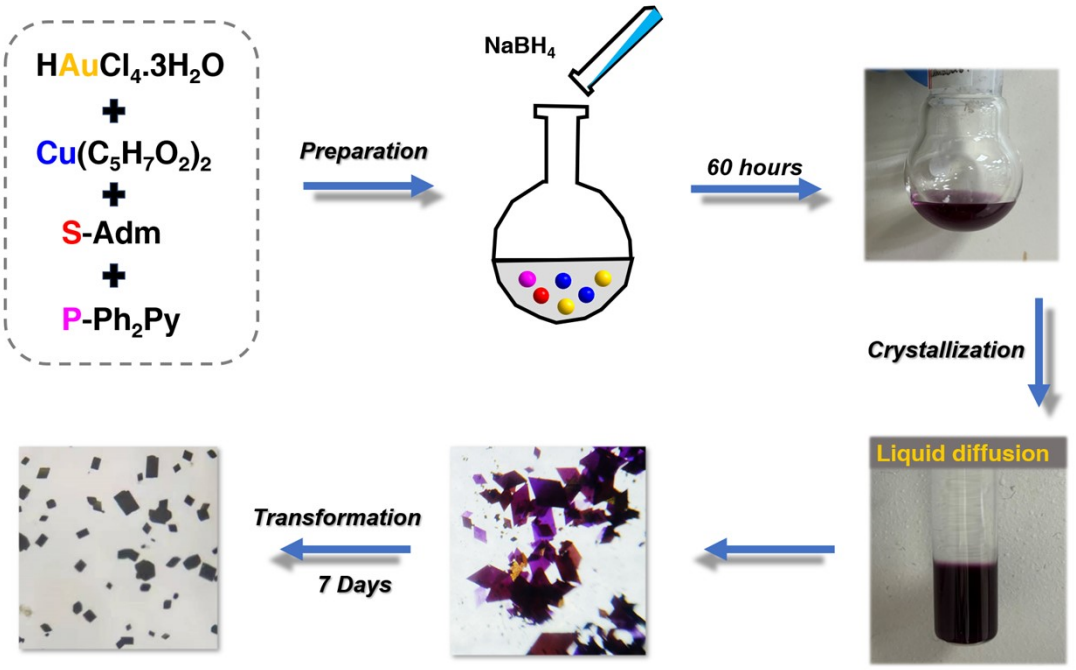

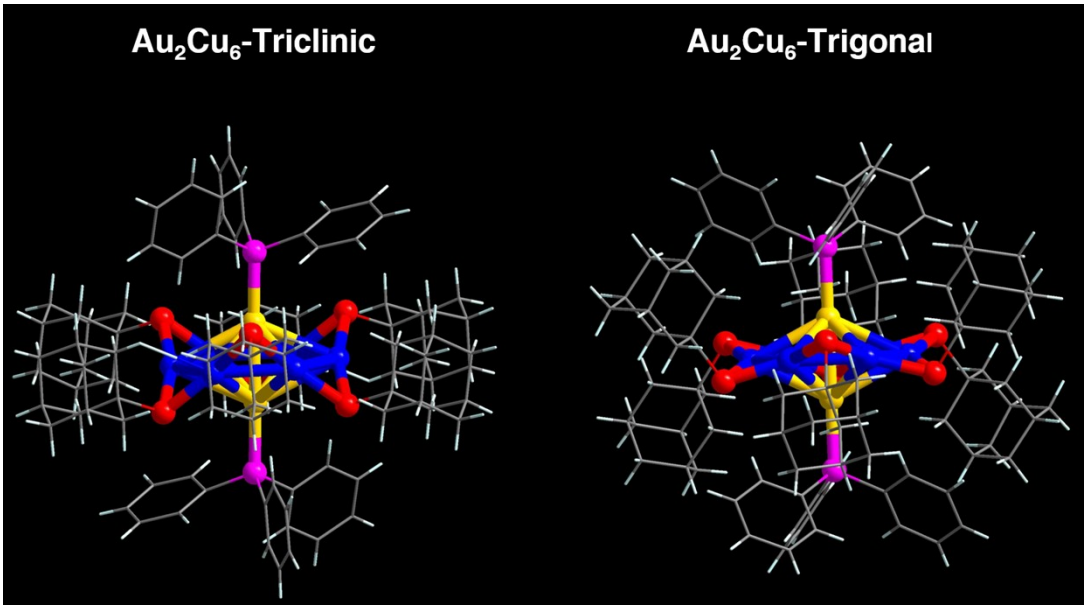

Figure S1. Overall structures of Au_2Cu_6-Triclinic and Au_2Cu_6-Trigonal nanoclusters. Color labels: orange = Au; blue = Cu; red = S; magenta = P; grey = C; white = H.

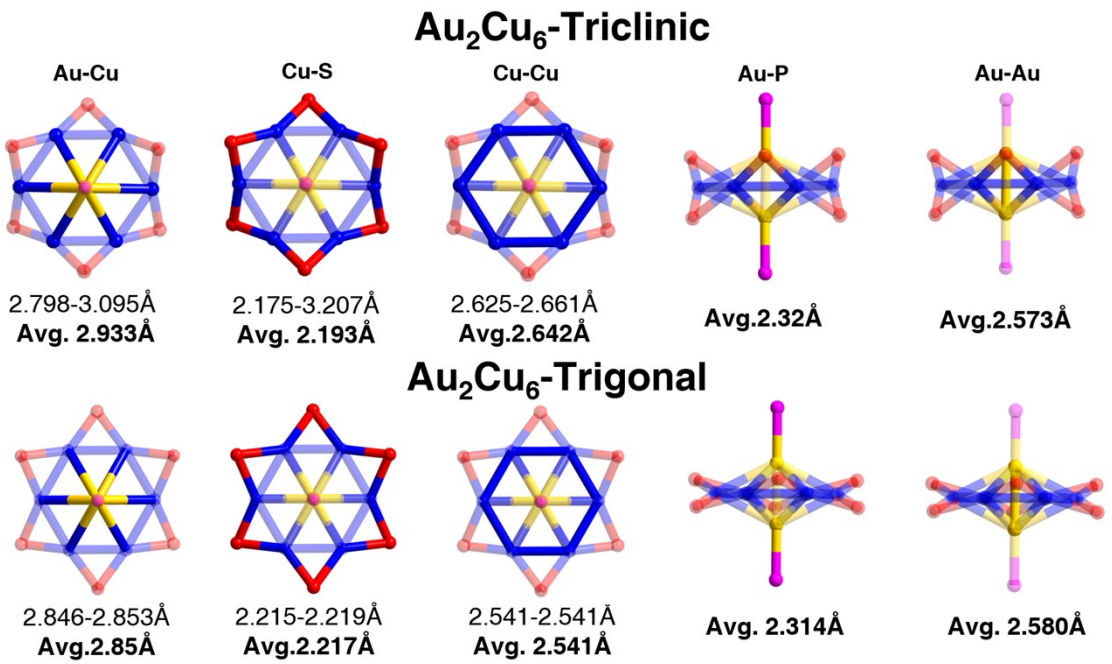

Figure S2. Comparison of the corresponding bond lengths of Au_2Cu_6-Triclinic and Au_2Cu_6-Trigonal nanoclusters, including Au-Cu, Cu-S, Cu-Cu, Au-P, and Au-Au bonds.

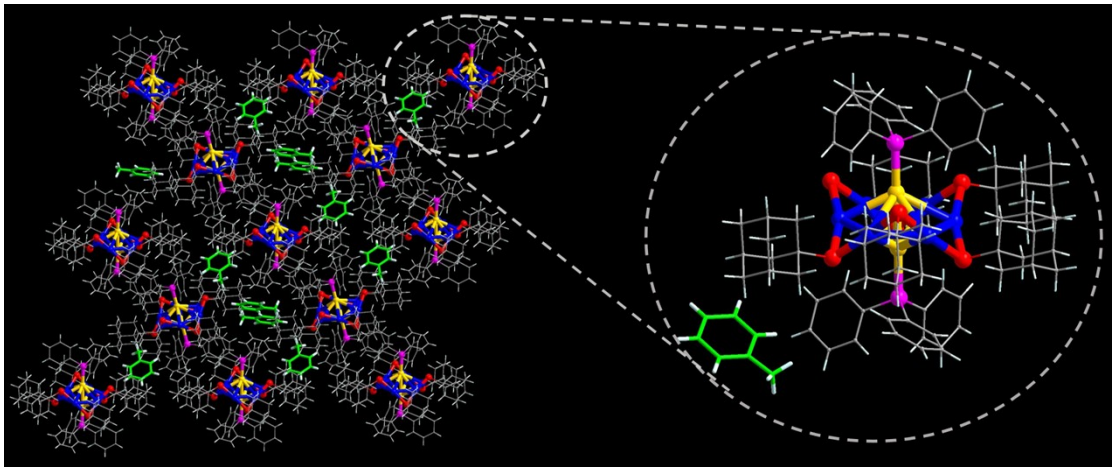

Figure S3. A unique toluene molecule was observed in the crystalline lattice of Au_2Cu_6-Triclinic, and the mole ratio of Au_2Cu_6-Triclinic cluster molecule/toluene molecule in the crystalline lattice is 1:1. Color labels: orange = Au; blue = Cu; red = S; magenta = P; grey = C in cluster molecules; green = C in toluene molecules; white = H.

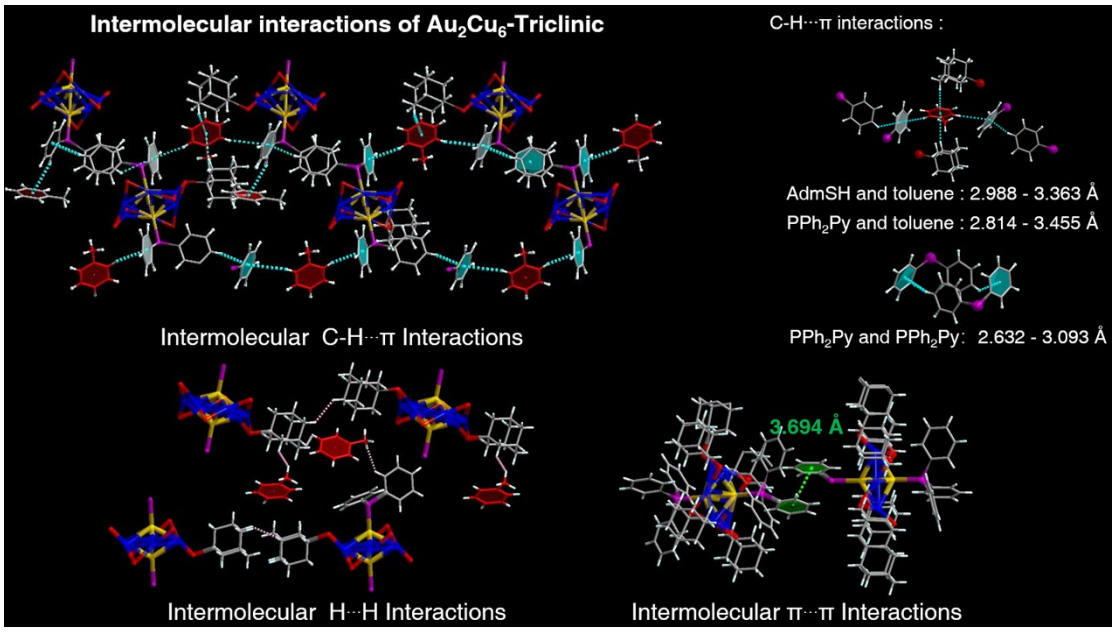

Figure S4. Due to the presence of the toluene molecule, several intermolecular C-H···π, H···H, and π···π interactions were detected in the crystal lattice of Au_2Cu_6-Triclinic. Color labels: orange = Au; blue = Cu; red = S; magenta = P; grey = C in cluster molecules; dark red = C in toluene molecules; white = H.

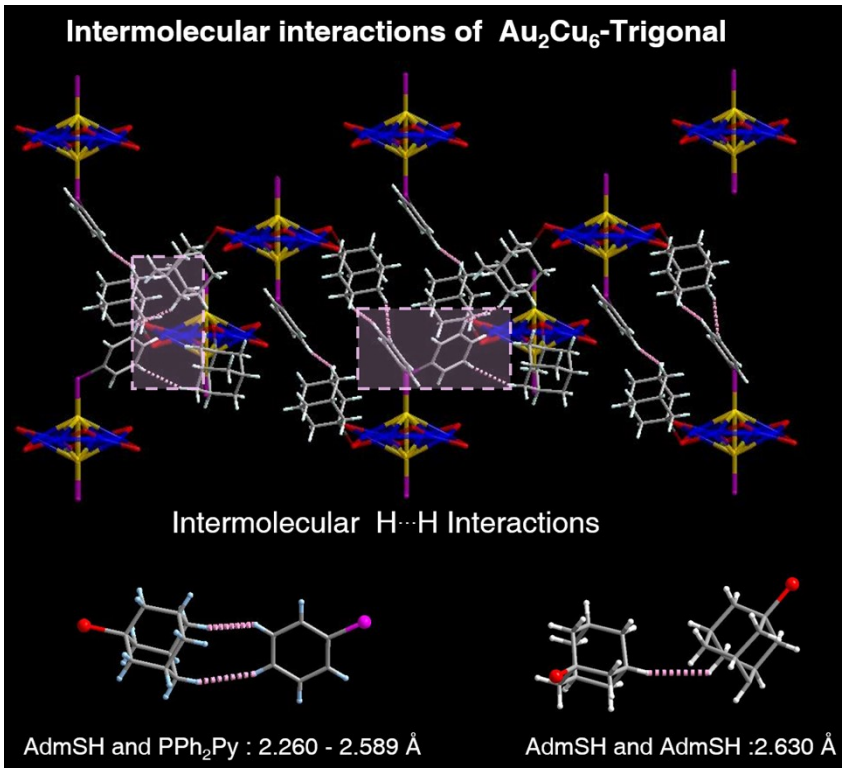

Figure S5. Weak H···H interactions in Au_2Cu_6-Trigonal. Color labels: orange = Au; blue = Cu; red = S; magenta = P; grey = C; white = H.

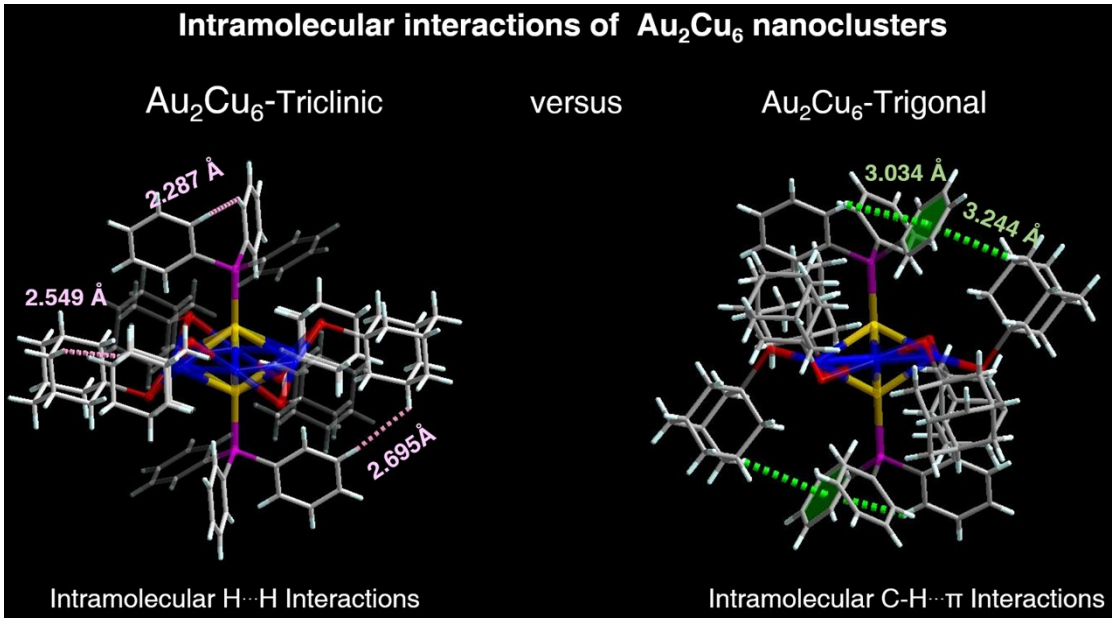

Figure S6. Intramolecular C-H$\cdots\pi$ or H$\cdots$H interactions in Au_2Cu_6 nanoclusters. Color labels: orange = Au; blue = Cu; red = S; magenta = P; grey = C; white = H. Pink labels: intramolecular H$\cdots$H interactions in Au_2Cu_6-Triclinic. Green labels: intramolecular C-H$\cdots\pi$ interactions in Au_2Cu_6-Trigonal.

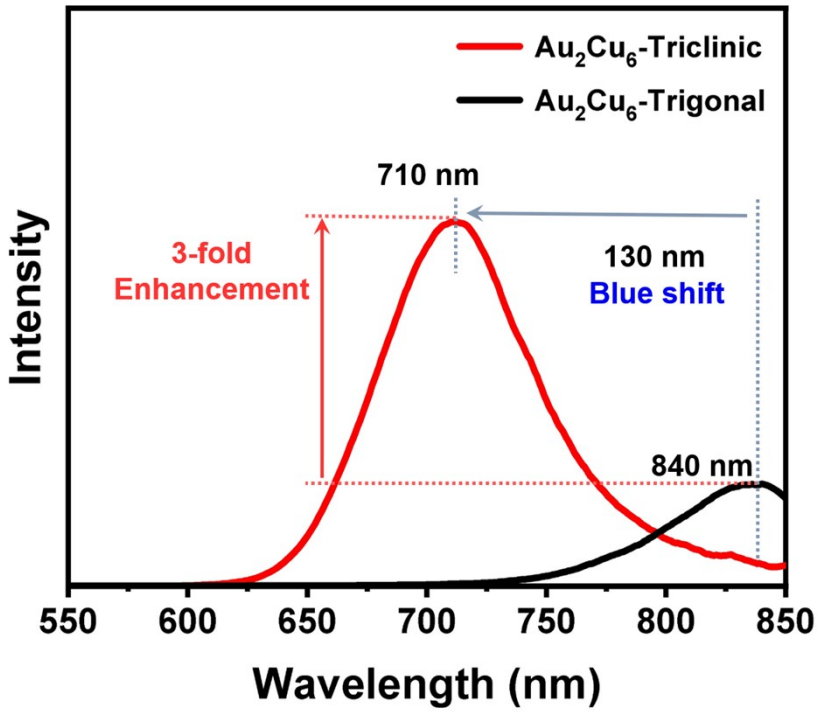

Figure S7. Comparison of the photoluminescence of the two Au_2Cu_6 nanocluster crystals. Black line: photoluminescence spectrum of Au_2Cu_6-Trigonal. Red line: photoluminescence spectrum of Au_2Cu_6-Triclinic. A 130 nm blue-shift on emission wavelength and a 3-fold enhancement on photoluminescence intensity were observed by comparing the emission of Au_2Cu_6-Triclinic to Au_2Cu_6-Trigonal.

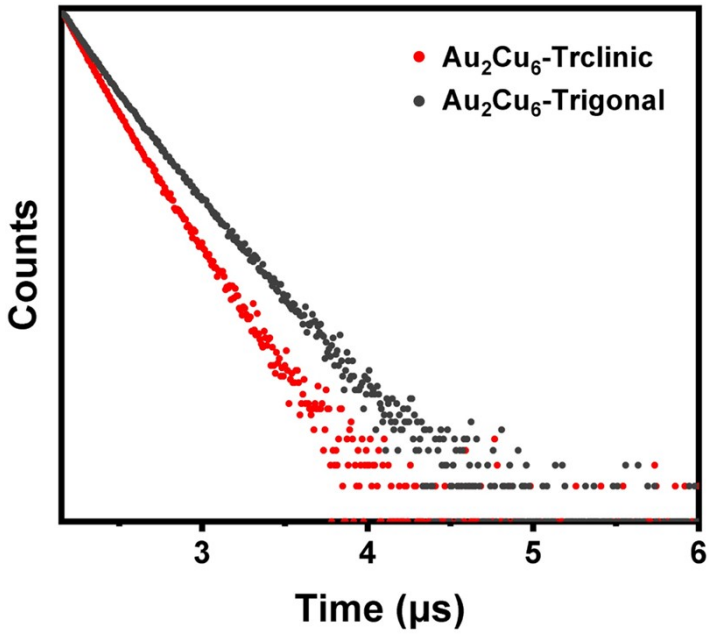

Figure S8. The PL lifetime of Au_2Cu_6-Triclinic (1.747 μs) was slightly shorter than that of Au_2Cu_6-Trigonal (2.209 μs). Black line: photoluminescence decay of Au_2Cu_6-Trigonal. Red line: photoluminescence decay of Au_2Cu_6-Triclinic.

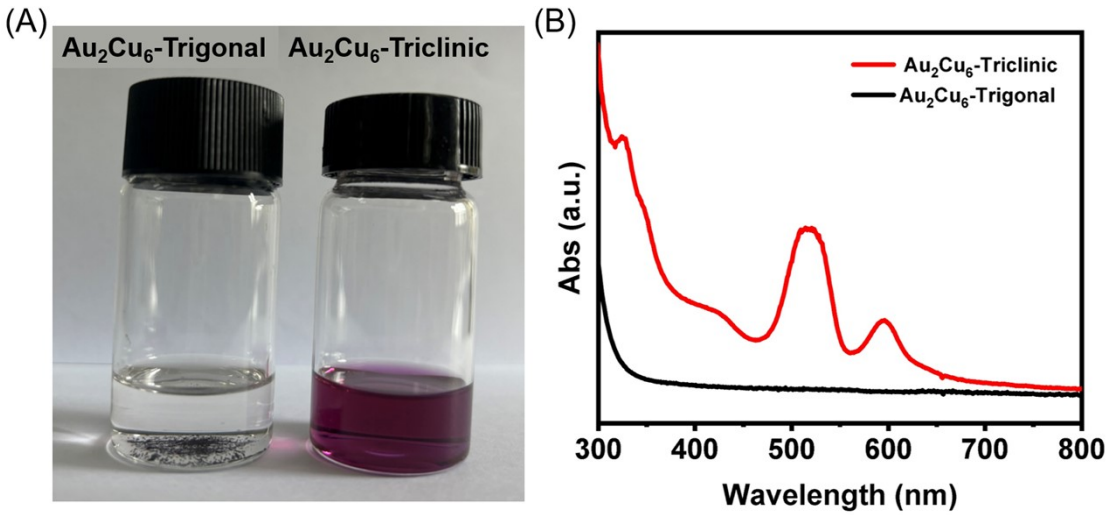

Figure S9. (A) The Au_2Cu_6-Triclinic crystals displayed good solubility in CH_2Cl_2, while the Au_2Cu_6-Trigonal was almost insoluble. Crystals of Au_2Cu_6-Triclinic also displayed good solubility in $CHCl_3$, toluene, and tetrahydrofuran, and their optical absorptions were the same as that of CH_2Cl_2. By comparison, the Au_2Cu_6-Trigonal crystals were insoluble in such solutions. (B) The optical absorptions of the CH_2Cl_2 solutions of the cluster crystals, which further suggested the good solubility of Au_2Cu_6-Triclinic and the insolubility of Au_2Cu_6-Trigonal.

Table S1. Crystal data and structure refinement for the Au_2Cu_6-Triclinic nanocluster. The CCDC number of the Au_2Cu_6-Triclinic nanocluster is 2347499.

Molecular formula	$C_{110}H_{136}Au_2Cu_6N_2P_2S_6$
Crystal system	triclinic
Space group	*P*-1
a/Å	15.244(10)
b/Å	18.456(12)
c/Å	18.809(7)
α/°	74.97(4)
β/°	82.45(4)
γ/°	88.26(5)
Volume/Å^3	5066(5)
Z	2
ρ_{calc}g/cm^3	1.631
μ/mm-1	8.455
F(000)	2508.0
Radiation	CuK\a (λ = 1.54186)
Index ranges	-17 ≤ h ≤ 12, -21 ≤ k ≤ 18, -21 ≤ l ≤ 21
2θ range (°)	9.926 to 124.998
Measured reflections and unique reflections	33167 [R_{int} = 0.0493, R_{sigma} = 0.0741]
Goodness-of-fiton F^2	0.949
Largest diff. peak/hole / e Å^{-3}	2.71/-1.53
Final R indexes [I>=2σ (I)]	R_1 = 0.0483, wR_2 = 0.1164
Final R indexes [all data]	R_1 = 0.0658, wR_2 = 0.1219

Table S2. Crystal data and structure refinement for the Au_2Cu_6-Trigonal nanocluster. The CCDC number of the Au_2Cu_6-Trigonal nanocluster is 2347507.

Molecular formula	$C_{96}H_{120}Au_2Cu_6P_2S_6$
Crystal system	trigonal
Space group	*R*-3
a/Å	21.0039(6)
b/Å	21.0039(6)
c/Å	18.0081(6)
α/°	90
β/°	90
γ/°	120
Volume/Å^3	6880.2(5)
Z	3
ρ_{calc}g/cm^3	1.668
μ/mm-1	9.284
F(000)	3462.0
Radiation	CuK\a (λ = 1.54186)
Index ranges	-24 ≤ h ≤ 16, -19 ≤ k ≤ 23, -20 ≤ l ≤ 13
2θ range (°)	13.788 to 124.994
Measured reflections and unique reflections	4428 [R_{int} = 0.0287, R_{sigma} = 0.0316]
Goodness-of-fiton F^2	1.154
Largest diff. peak/hole / e Å^{-3}	1.34/-2.04
Final R indexes [I>=2σ (I)]	R_1 = 0.0386, wR_2 = 0.1064
Final R indexes [all data]	R_1 = 0.0419, wR_2 = 0.1260